https://doi.org/10.5194/egusphere-2023-1560
Preprint. Discussion started: 26 July 2023
© Author(s) 2023. CC BY 4.0 License.

Brief Communication

On the mid-summer melt pond fraction–September Arctic sea ice extent relationship in the EC-Earth3 climate model

Mukesh Gupta[1], Leandro Ponsoni[1,2], Jean Sterlin[1], François Massonnet[1], Thierry Fichefet[1]

[1]Earth and Climate Centre, Earth and Life Institute (ELI), Université catholique de Louvain, Louvain-la-Neuve, Belgium
[2]Marine Robotics Centre (MRC), Flanders Marine Institute (VLIZ), Ostend, Belgium

Correspondence to: Mukesh Gupta (guptm@yahoo.com)

Abstract. In a recent study, the springtime melt pond fraction has been suggested to be a predictor of subsequent September Arctic sea ice minimum extent anomalies. However, another study based on satellite data did not provide evidence for such a relationship. We explore this association in EC-Earth3, which includes an explicit treatment of melt ponds, for the present-day climate. We find a statistically significant inverse relationship between September sea ice extent and mid-summer (June-July) melt pond fraction on the seasonal scale. Our results support the satellite-based inferences that the mid-summer melt pond fraction highly correlates with the September ice extent.

1 Introduction

Melt ponds are pools of water formed at the sea ice surface when snow and ice melt. The typical albedo of well-developed melt ponds is about 0.13 versus 0.85 for cold snow over sea ice (see, e.g., Grenfell and Perovich, 2004). By reducing the surface albedo locally, melt ponds have thus a strong impact on the surface energy balance and, ultimately, on the sea ice mass balance. Melt pond formation can enhance sea ice melting and potentially lead to more ponds, creating a positive feedback loop (Taylor and Feltham, 2004; Schröder et al., 2014). Thus, despite the short duration of the melt pond season in the Arctic, which extends mainly from May through September, melt ponds potentially exert a key control on the seasonal retreat of the Arctic sea ice cover and on the spatial distribution of sea ice that remains at the summer minimum, in September. Accounting for their presence in numerical models is therefore of importance, especially in long-term Arctic climate projections. Currently, most global climate models account for melt ponds only implicitly, e.g., by tuning the sea ice albedo. To our knowledge, some models of this type that include melt ponds implicitly are CNRM-CM5 (Voldoire et al., 2013), NorESM1-M (Sandø et al., 2014), and HadGEM-GC3 (Williams et al., 2018).

Three studies have inspected the relationship between Arctic melt pond fraction and September sea ice minimum extent. First, Schröder et al. (2014) used a stand-alone sea ice model forced with atmospheric reanalysis data to conclude that

https://doi.org/10.5194/egusphere-2023-1560
Preprint. Discussion started: 26 July 2023
© Author(s) 2023. CC BY 4.0 License.

it is possible to predict the September ice extent using the May melt pond fraction as a predictor. Second, Liu et al. (2015) used independent observational data and came to different conclusions. They argued that a significant relationship between satellite-based melt pond fraction and September ice extent only emerges when the melt pond fraction is integrated from early May to late June, with a persistent strong relationship only occurring after integrating July. Liu et al. suggested no evidence of predictive skill stemming from May melt ponds only. A recent study (Feng et al., 2022) reaffirmed the satellite-based assessment, showing that the integrated melt pond fraction exhibits the strongest correlation with satellite-derived September sea ice extent in June but not before that month.

The objective of this paper is to shed light on the above conundrum with a fourth independent and complementary perspective. We investigate the possible statistical relationship between the spring-summer melt pond fraction area anomalies and the September Arctic sea ice extent using a global climate model, which includes an explicit melt ponds scheme, under the constant forcing of the fix-year 2000 CE that represents the present-day climate. The advantage of this approach is that global climate models permit interactions between the ocean-sea ice and atmosphere (the limitation of the Schröder et al. 2014 study) and allow examining the internal associations between melt pond area fraction and ice extent under constant forcing regardless of the changing mean state, thus excluding the role of confounding factors. In addition, the relatively long integration time of the model brings improved statistical robustness to this analysis.

2 Methods

We have implemented the topographic scheme of Flocco and Feltham (2007) and Flocco et al. (2010) in the PRIMAVERA (PRocess-based climate sIMulation: AdVances in high-resolution modeling and European climate Risk Assessments) [r4796, revision 5888] version of the third generation of the European Community Earth System Model (EC-Earth3) to study the Arctic melt pond evolution (Ponsoni et al., 2021; Döscher et al., 2022; Ortega et al., 2022). EC-Earth3 comprises the atmospheric model Integrated Forecasting System (IFS), development cycle 36r4, and the Nucleus for European Modelling of the Ocean (NEMO) modelling framework version 3.6, which includes the Louvain-la-Neuve Sea Ice Model 3 (LIM3) (Rousset et al., 2015; Tian et al., 2021). The albedo scheme in the ocean-covered grid cells of the model considers the contributions from the ocean, ice, snow, and melt ponds, weighted by their respective areas. The melt pond albedo varies with the pond depth. LIM3 sea ice model incorporates a discrete ice thickness distribution, here using five categories. The fraction f of the fluxes of melting snow and ice (at the surface) that enter the melt ponds varies with the ice concentration per ice category A_i as $f(A_i) = 0.15 + 0.55A_i$. Using a category-dependent scheme for distributing meltwater avoids prescribing unphysical fluxes, like meltwater on very thin ice. The model calculates the surface meltwater volume from the snow and ice thickness changes due to melting at each time step. The volume of meltwater in the ponds is redistributed among the ice categories according to Flocco and Feltham (2007).

Our configuration of EC-Earth3 uses the ORCA1L75 grid, which is a tripolar grid with a nominal resolution of 1º and 75 vertical ocean levels. The global grid in the atmosphere is T255L91, which corresponds to a ~80 km horizontal

https://doi.org/10.5194/egusphere-2023-1560
Preprint. Discussion started: 26 July 2023
© Author(s) 2023. CC BY 4.0 License.

resolution with 91 vertical levels. Specific to the PRIMAVERA version, the simulation uses a simplified CMIP6 stratospheric aerosol forcing from the Goddard Institute for Space Studies (GISS) volcanic dataset (Johansson et al., 2021). Spatio-temporal evolution of melt ponds is obtained from 105 years of a 200-year-long experiment (spin-up = 95 years) under a constant forcing (Fig. 1a). The IFS model (EC-Earth3) treats orbital forcing-related parameters as constants and the fix-year 2000 CE levels of greenhouse gas forcing for the present-day climate. We have omitted the first 95 years because of the strong model drift, leading to a statistically insignificant correlation between ice extent and melt pond fraction during this period. Within the limits of statistically significant correlations following the spin-up period, we assume that the model achieved stability despite persistent variability. An advantage of constant forcing simulations is that we exclude the possibility that time-varying greenhouse gas forcing drives both the melt pond area fraction and sea ice extent so that, if there is a melt pond fraction-ice extent relationship, it is more likely to be a causal than when derived from other types of greenhouse gas forcing scenarios.

We use a consistent time series of September minimum ice extent for 42 years (1979 to 2020) from the Special Sensor Microwave/Imager (SSM/I) and several other passive microwave instruments to compare with model results (Cavalieri et al., 1996). To validate the modelled melt pond fraction, we utilise the monthly Moderate Resolution Imaging Spectroradiometer (MODIS) satellite data products provided by Lee et al. (2020) and Rösel et al. (2012). Rösel et al. (2012) generated the multi-annual melt pond fraction product for the entire Arctic from the Level-3 MODIS surface reflectance using an artificial neural network. Lee et al. (2020) applied a multi-layer neural network and multinomial logistic regression to retrieve pan-Arctic binary melt pond fraction from the normalized band difference of MODIS reflectance.

[Figure 1 near here]

3 Results and Discussion

3.1 Model Evaluation

The simulated and observed sea ice extents are expected to differ from each other in obvious ways since the observed one is under the influence of a transient forcing from 1979 to 2020, while the simulated one assumes a time-invariant forcing. Nevertheless, we can evaluate the model output with basic metrics, such as the integrated sea ice extent to obtain a general idea of the model's ability to reproduce the observed state. Table 1 shows the mean state and variability of the observed September sea ice extent from 1979 to 2020 and the modelled sea ice extent for the selected years of EC-Earth3 simulation. Although it is difficult to compare outputs generated from different forcings, it is clear from Table 1 that the modelled mean (N = 105) is 12% of the observed mean (N = 42) and the minimum-maximum range is overestimated. The variability in the model output (constant forcing) is 23% higher than the observed variability (transient state) (Table 1). It may be because of unexplained factors beyond this research.

[Table 1 near here]

https://doi.org/10.5194/egusphere-2023-1560
Preprint. Discussion started: 26 July 2023
© Author(s) 2023. CC BY 4.0 License.

The model outputs exhibit a distinct relationship between the integrated melt pond area fraction (per unit sea ice area) and September total sea ice extent (Fig. 1b). In the current context, our model results produced statistically significant relationships (Fig. 1b, discussed in Sect. 3.2).

Figure 1d shows the evaluation of modelled melt pond fraction against the observed melt pond fraction using data provided by Lee et al. (2020) and Rösel et al. (2012). Monthly melt pond fraction data by Lee et al. (2020) are from 2000 to 2019 and that by Rösel et al. (2012) from 2000 to 2011. Because all melt pond fraction data are monthly, it is difficult to get the exact date of melt pond onset in the model output and observations. However, the timing of the melt pond development is broadly consistent between the model and observations. Except for July, the model slightly underestimates the pond fraction, with an overall good correlation (Pearson's *r*) of 0.85 (Lee) and 0.96 (Rösel) with the modelled pond fraction (Fig. 1d). The melt pond results of our EC-Earth3 simulation are consistent with the melt pond observations for the period from 2000 to 2019 based on various satellite data products and model results based on the ocean-sea ice model (NEMO3.6-LIM3) (Sterlin et al., 2021).

3.2. Relationship between Sea Ice Extent and Melt Pond Fraction

In the model results and observations, melt ponds appear in the Arctic in May and mostly disappear in September, reaching their peak towards the end of July (Liu et al., 2015) (Fig. 2a). The simulated melt pond fraction reaches its maximum during July with a mean value above 0.33, closely matching the observed values (Figs. 2a and 1d). The statistical relationship between the modelled September ice extent and simulated melt pond fraction is weak in May because of the small melt pond fraction but gets stronger and more significant as mid-summer approaches (Fig. 2b).

[Figure 2 near here]

Figure 3 shows the spatial distribution of correlation between the simulated mean melt pond area fraction (integrated from May through July) and the corresponding September sea ice extent. The magenta line represents the modelled mean September sea ice extent. The geographical distribution of grid points where correlation is statistically significant varies between Schröder et al. (2014), Liu et al. (2015) and our study. Schröder et al. found strong correlations in the Baffin Bay, the Canada Basin, the Amerasian Basin, and the Eurasian Basin [see Fig. 2a by Schröder et al. (2014)]. Liu et al. reported statistically significant correlations in the region between the Canada Basin and the central Arctic Ocean [see Fig. 2b by Liu et al. (2015)]. Our study shows the strongest correlations in the Fram Basin and Nansen Basin regions of the central Arctic Ocean [Fig. 3b, d, and f]. Figure 3 shows an increasing and varying correlation, starting from May through July. This disparity is likely because of systematic errors (biases) and a varying temporal gap between different model outputs; Schröder et al. used daily model output, Liu et al. (2015) used 8-day interval melt pond fraction observations, and our study relies on the monthly output of EC-Earth3. Liu et al. (2015) reported that satellite observations exhibit a much higher percentage of May melt pond fraction than does the forced model output given by Schröder et al. (2014).

https://doi.org/10.5194/egusphere-2023-1560
Preprint. Discussion started: 26 July 2023
© Author(s) 2023. CC BY 4.0 License.

A significant statistical relationship exists between the anomalies of the simulated September ice extent and the modelled integrated (May through July) melt pond fraction with Pearson's correlation coefficient $r = -0.76$ for the selected years of simulation (Fig. 1b). It is clear from Fig. 1c that the observed mid-summer pond fraction anomaly (percentage) has a significant inverse correlation (Lee: $r = -0.60$, p-value = 0.006; Rösel: $r = -0.73$, p-value = 0.007) with the SSM/I September ice extent anomaly (percentage). This satellite-based strong negative statistical relationship between mid-summer melt pond fraction and September ice extent agrees with conclusions by Liu et al. (2015) and our model results confirm these observed relationships. Changing the frequency of the model output from monthly to daily may further improve the computed correlation.

[Figure 3 near here]

The results share several of the conclusions of Schröder et al. (2014) who predicted a relationship between September sea ice extent and the May melt pond area fraction in a stand-alone sea ice model. However, the results from our coupled model show a weaker relationship than in their study and support the conclusions made by Liu et al. (2015), who stated that the September ice extent strongly correlates with the mid-summer melt pond fraction, whereas the correlation in May is not as strong as it is in mid-summer.

4 Conclusions

This paper explored the relationship of September sea ice extent in the Arctic with mid-summer melt pond area fraction, under the constant greenhouse gas forcing for the fix-year 2000 CE. Under the assumption that the model attained stability in the run (see Sect. 2 for details), we find a statistically significant inverse relationship between September sea ice extent and integrated (May through July) melt pond fraction on the seasonal scale. Our results support the satellite-based inferences made by Liu et al. (2015) and Feng et al. (2022) that the mid-summer (June-July) pond fraction highly correlates with the September sea ice extent suggesting limited predictability stemming from this variable at a 5-month lead time.

The work presented here cross-verified the degree of predictive skill of a stand-alone sea ice model forced with atmospheric reanalysis data for predicting September sea ice extent from melt pond area fraction (Schröder et al., 2014). Based on our findings, it is worthwhile to deduce that the degree of predictive skill may increase if mid-summer replaces the early spring (May) melt pond fraction.

Code Availability

Selected codes may be available upon request.

https://doi.org/10.5194/egusphere-2023-1560
Preprint. Discussion started: 26 July 2023
© Author(s) 2023. CC BY 4.0 License.

Data Availability

Model simulation data are available upon request. Melt pond observations data are available at https://www.cen.uni-hamburg.de/ and http://www.cpom.ucl.ac.uk/melt_pond/. SSM/I sea ice extent data are available at https://doi.org/10.5067/8GQ8LZQVL0VL.

Author Contribution

MG performed the experiments, analyzed the data, created figures, and wrote the manuscript. JS coded the melt pond parameterization, tested its performance for accuracy, and provided validation datasets. LP examined and helped design the experiments. FM and TF supervised the work and arranged the funding. All authors contributed to the conceptualization and edited the manuscript.

Competing Interests

The authors declare they have no conflict of interest.

Acknowledgements

The work presented in this paper has received funding from the European Union's Horizon 2020 Research & Innovation programme under grant agreement No. 727862 (APPLICATE Project–Advanced Prediction in Polar regions and beyond: Modelling, observing system design and LInkages associated with a Changing Arctic climaTE). LP (and FM) was (is) funded by the Fond de la Recherche Scientifique de Belgique (F.R.S.-FNRS). The authors thank Pierre-Yves Barriat for his help with the technical explanations of various components of EC-Earth3. Computational resources have been provided by the supercomputing facilities of the Université catholique de Louvain (CISM/UCL) and the Consortium des Équipements de Calcul Intensif en Fédération Wallonie Bruxelles (CÉCI) funded by F.R.S.-FNRS under convention 2.5020.11 and by the Walloon Region. The present research benefited from computational resources made available on the Tier-1 supercomputer of the Fédération Wallonie-Bruxelles, infrastructure funded by the Walloon Region under the grant agreement n°1117545.

https://doi.org/10.5194/egusphere-2023-1560
Preprint. Discussion started: 26 July 2023
© Author(s) 2023. CC BY 4.0 License.

References

Döscher, R., Acosta, M., Alessandri, A., Anthoni, P., Arsouze, T., Bergman, T., Bernardello, R., Boussetta, S., Caron, L. -P., Carver, G., Castrillo, M., Catalano, F., Cvijanovic, I., Davini, P., Dekker, E., Doblas-Reyes, F. J., Docquier, D., Echevarria, P., Fladrich, U., Fuentes-Franco, R., Gröger, M., v. Hardenberg, J., Hieronymus, J., Karami, M. P., Keskinen, J. -P., Koenigk, T., Makkonen, R., Massonnet, F., Ménégoz, M., Miller, P. A., Moreno-Chamarro, E., Nieradzik, L., van Noije, T., Nolan, P., O'Donnell, D., Ollinaho, P., van den Oord, G., Ortega, P., Prims, O. T., Ramos, A., Reerink, T., Rousset, C., Ruprich-Robert, Y., Le Sager, P., Schmith, T., Schrödner, R., Serva, F., Sicardi, V., Sloth Madsen, M., Smith, B., Tian, T., Tourigny, E., Uotila, P., Vancoppenolle, M., Wang, S., Wårlind, D., Willén, U., Wyser, K., Yang, S., Yepes-Arbós, X., and Zhang, Q.: The EC-Earth3 Earth system model for the Coupled Model Intercomparison Project 6, Geosci. Model Dev., 15, 2973–3020, doi:10.5194/gmd-15-2973-2022, 2022.

Feng, J., Zhang, Y., Cheng, Q., and Tsou, J. Y.: Pan-Arctic melt pond fraction trend, variability, and contribution to sea ice changes, Glob. Planet. Change, 217, 103932, doi:10.1016/j.gloplacha.2022.103932, 2022.

Flocco, D. and Feltham, D. L.: A continuum model of melt pond evolution on Arctic sea ice, J. Geophys. Res.: Oceans, 112, C8, doi:10.1029/2006JC003836, 2007.

Flocco, D., Feltham, D. L., and Turner, A.K.: Incorporation of a physically based melt pond scheme into the sea ice component of a climate model, J. Geophys. Res.: Oceans, 115, C8, doi:10.1029/2009JC005568, 2010.

Grenfell, T. C. and Perovich, D. K.: Seasonal and spatial evolution of albedo in a snow-ice-land-ocean environment, J. Geophys. Res.: Oceans, 109, C1, doi:10.1029/2003JC001866, 2004.

Johansson, E., Devasthale, A., Tjernström, M., Ekman, A. M. L., Wyser, K., and L'Ecuyer, T.: Vertical structure of cloud radiative heating in the tropics: confronting the EC-Earth v3.3.1/3P model with satellite observations, Geosci. Model Dev., 14, 4087–4101, doi:10.5194/gmd-14-4087-2021, 2021.

Lee, S. and Stroeve, J.: Arctic Melt Pond Fraction and Binary Classification, 2000-2020 (Version 1.0). UK Polar Data Centre, Natural Environment Research Council, UK Research & Innovation, doi:10.5285/B91EA195-FD3D-4171-BAE4-198C46575C16, 2021.

Lee, S., Stroeve, J., Tsamados, M., and Khan, A. L.: Machine learning approaches to retrieve pan-Arctic melt ponds from visible satellite imagery, Remote Sens. Environ., 247, 111919, doi:10.1016/j.rse.2020.111919, 2020.

https://doi.org/10.5194/egusphere-2023-1560
Preprint. Discussion started: 26 July 2023
© Author(s) 2023. CC BY 4.0 License.

Liu, J., Song, M., Horton, R. M., and Hu, Y. Revisiting the potential of melt pond fraction as a predictor for the seasonal Arctic sea ice extent minimum, Environ. Res. Lett., 10, 054017, doi:10.1088/1748-9326/10/5/054017, 2015.

Ortega, P., Blockley, E. W., Koltzow, M., Massonnet, F., Sandu, I., Svensson, G., Acosta Navarro, J. C., Arduini, G., Batte, L., Bazile, E., Chevallier, M., Cruz-Garcia, R., Day, J. J., Fichefet, T., Flocco, D., Gupta, M., Hartung, K., Hawkins, E., Hinrichs, C., Magnusson, L., Moreno-Chamarro, E., Perez-Montero, S., Ponsoni, L., Semmler, T., Smith, D., Sterlin, J., Tjernstrom, M., Valisuo, I., and Jung, T.: Improving Arctic weather and seasonal climate prediction: Recommendations for future forecast systems evolution from the European Project APPLICATE, Bull. Am. Meteorol. Soc., 103, E2203–E2213. doi:10.1175/BAMS-D-22-0083.1, 2022.

Ponsoni, L., Gupta, M., Sterlin, J., Massonnet, F., Fichefet, T., Hinrichs, C., Semmler, T., Arduini, G., Ridley, J., Nummelin, A., Msadek, R., Terray, L., Salas y Melia, D., Svensson, G., and Blockley, E.: Deliverable No. 2.5 Final report on model developments and their evaluation in coupled mode. APPLICATE WP2, H2020 - Research and Innovation Action, Work Package 2: Enhanced weather and climate models. pp. 78. Zenodo. doi:10.5281/zenodo.4916934, 2021.

Rösel, A., Kaleschke, L., and Birnbaum, G.: Melt ponds on Arctic sea ice determined from MODIS satellite data using an artificial neural network, Cryosphere, 6, 431–446, doi:10.5194/tc-6-431-2012, 2012.

Rousset, C., Vancoppenolle, M., Madec, G., Fichefet, T., Flavoni, S., Barthélemy, A., Benshila, R., Chanut, J., Lévy, C., Masson, S., and Vivier, F.: The Louvain-La-Neuve sea ice model LIM3.6: global and regional capabilities, Geosci. Model Dev., 8, 2991–3005, doi:10.5194/gmd-8-2991-2015, 2015.

Sandø, A. B., Gao, Y., and Langehaug, H. R.: Poleward ocean heat transports, sea ice processes, and arctic sea ice variability in NorESM1-M simulations, J. Geophys. Res.: Oceans, 119, 2095–2108, doi:10.1002/2013JC009435, 2014.

Schröder, D., Feltham, D. L., Flocco, D., and Tsamados, M.: September Arctic sea ice minimum predicted by spring melt pond fraction, Nat. Clim. Change, 4, 353–357, doi:10.1038/nclimate2203, 2014.

Sterlin, J., Fichefet, T., Massonnet, F., Lecomte, O., and Vancoppenolle, M.: Sensitivity of Arctic sea ice to melt pond processes and atmospheric forcing: A model study, Ocean Model., 167, 101872, doi:10.1016/j.ocemod.2021.101872, 2021.

Taylor, P. D. and Feltham, D. L.: A model of melt pond evolution on sea ice, J. Geophys. Res.: Oceans, 109, C12, doi:10.1029/2004JC002361, 2004.

https://doi.org/10.5194/egusphere-2023-1560
Preprint. Discussion started: 26 July 2023
© Author(s) 2023. CC BY 4.0 License.

Tian, T., Yang, S., Karami, M. P., Massonnet, F., Kruschke, T., and Koenigk, T.: Benefits of sea ice initialization for the interannual-to-decadal climate prediction skill in the Arctic in EC-Earth3, Geosci. Model Dev., 14, 4283–4305, doi:10.5194/gmd-14-4283-2021, 2021.

Voldoire, A., Sanchez-Gomez, E., Salas y Mélia, D., Decharme, B., Cassou, C., Sénési, S., Valcke, S., Beau, I., Alias, A., Chevallier, M., and Déqué, M.: The CNRM-CM5. 1 global climate model: description and basic evaluation, Clim. Dyn., 40, 2091–2121, doi:10.1007/s00382-011-1259-y, 2013.

Williams, K. D., Copsey, D., Blockley, E. W., Bodas-Salcedo, A., Calvert, D., Comer, R., Davis, P., Graham, T., Hewitt, H. T., Hill, R., and Hyder, P.: The Met Office global coupled model 3.0 and 3.1 (GC3. 0 and GC3. 1) configurations, J. Adv. Model. Earth Syst., 10, 357–380, doi:10.1002/2017MS001115, 2018.

https://doi.org/10.5194/egusphere-2023-1560
Preprint. Discussion started: 26 July 2023
© Author(s) 2023. CC BY 4.0 License.

List of Figure Captions

Figure 1: (a) Time series of September total sea ice extent and integrated (May through July) melt pond area fraction for a 200-year simulation using EC-Earth3. The vertical black line in the center represents the 95th year of simulation which corresponds to the beginning of the period analyzed in this paper. (b) Scatterplot and regression values between de-trended ice extent anomaly and de-trended melt pond fraction anomaly for the model. (c) Scatterplot and regression values between the observed de-trended ice extent anomaly (SSM/I) and the observed de-trended pond fraction anomaly (Lee et al., 2020 [N = 19], and Rösel et al., 2012 [N = 12]), and (d) a comparison of the modelled and observed temporal evolutions of the melt pond fraction.

Figure 2: (a) Time series of the modelled melt pond area fraction for May, June, July, and August. (b) Pearson's r (with 95% and 99% confidence intervals) between the de-trended time series of the simulated melt pond fraction (integration period from May to August) and modelled September sea ice extent (N = 105).

Figure 3: (Left column: a, c, and e) Spatial distribution of mean melt pond area fraction (May through July) from a 105-year simulation conducted with EC-Earth3. (Right column: b, d, and f) Corresponding spatial distribution of correlation between melt pond fraction and de-trended September ice extent (Pearson's $r < 0$) for the selected years of simulation (see Fig. 1a). The magenta line is the mean of modelled September sea ice extent.

https://doi.org/10.5194/egusphere-2023-1560
Preprint. Discussion started: 26 July 2023
© Author(s) 2023. CC BY 4.0 License.

Table 1: Comparison of mean state and variability of SSM/I September sea ice extent (1979 to 2020) and September ice extent for the last 105 years of EC-Earth3 simulation.

Metric	**SSM/I September sea ice extent (1979 to 2020) (10^6 km^2)**	**EC-Earth3 September sea ice extent (105 years of simulation) (10^6 km^2)**
Mean	5.09	4.47
Minimum	3.57	1.93
Maximum	6.73	7.25
Standard deviation	0.82	1.06

https://doi.org/10.5194/egusphere-2023-1560
Preprint. Discussion started: 26 July 2023
© Author(s) 2023. CC BY 4.0 License.

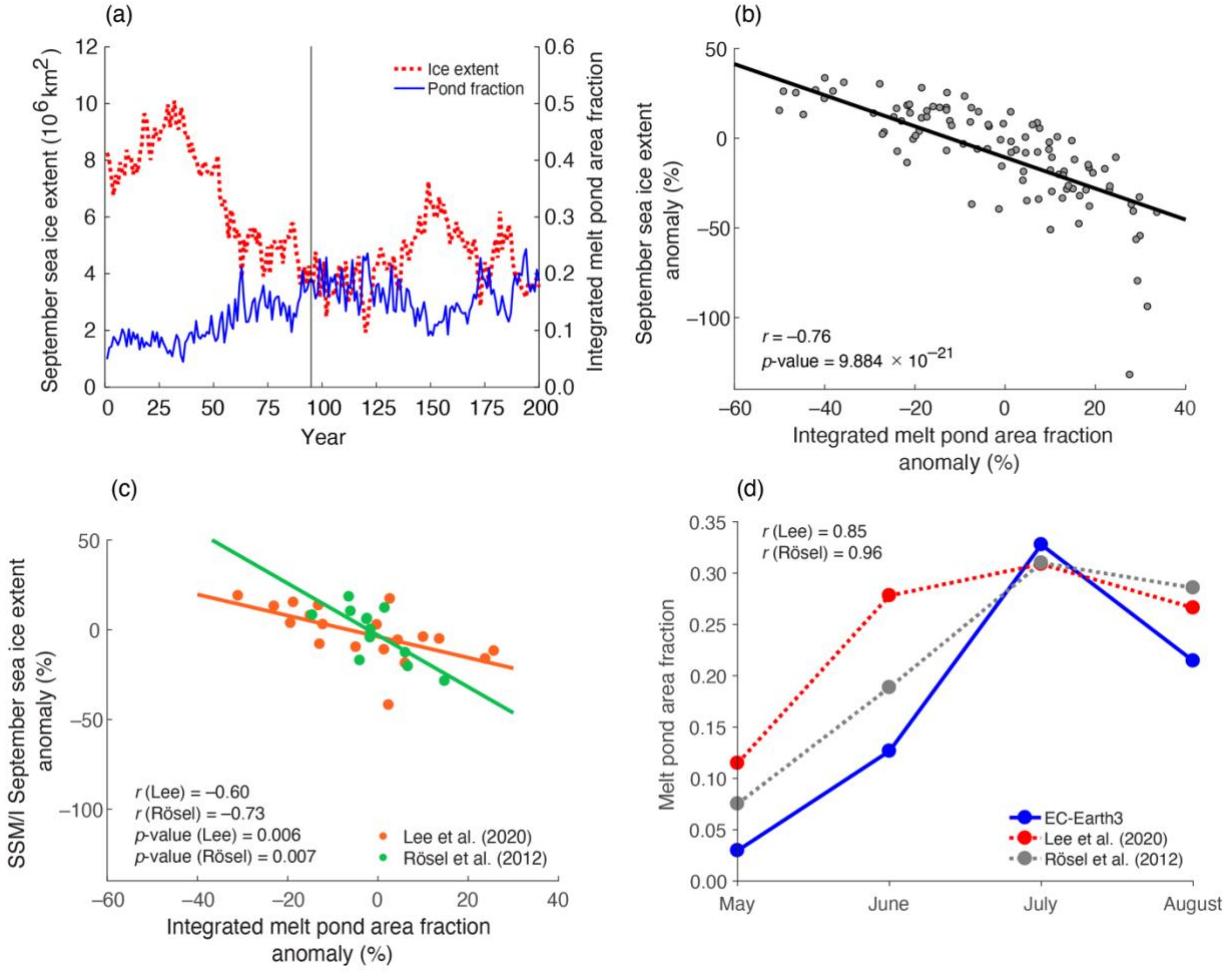

Figure 1: (a) Time series of September total sea ice extent and integrated (May through July) melt pond area fraction for a 200-year simulation using EC-Earth3. The vertical black line in the center represents the 95th year of simulation which corresponds to the beginning of the period analyzed in this paper. (b) Scatterplot and regression values between de-trended ice extent anomaly and de-trended melt pond fraction anomaly for the model. (c) Scatterplot and regression values between the observed de-trended ice extent anomaly (SSM/I) and the observed de-trended pond fraction anomaly (Lee et al., 2020 [*N* = 19], and Rösel et al., 2012 [*N* = 12]), and (d) a comparison of the modelled and observed temporal evolutions of the melt pond fraction.

https://doi.org/10.5194/egusphere-2023-1560
Preprint. Discussion started: 26 July 2023
© Author(s) 2023. CC BY 4.0 License.

290

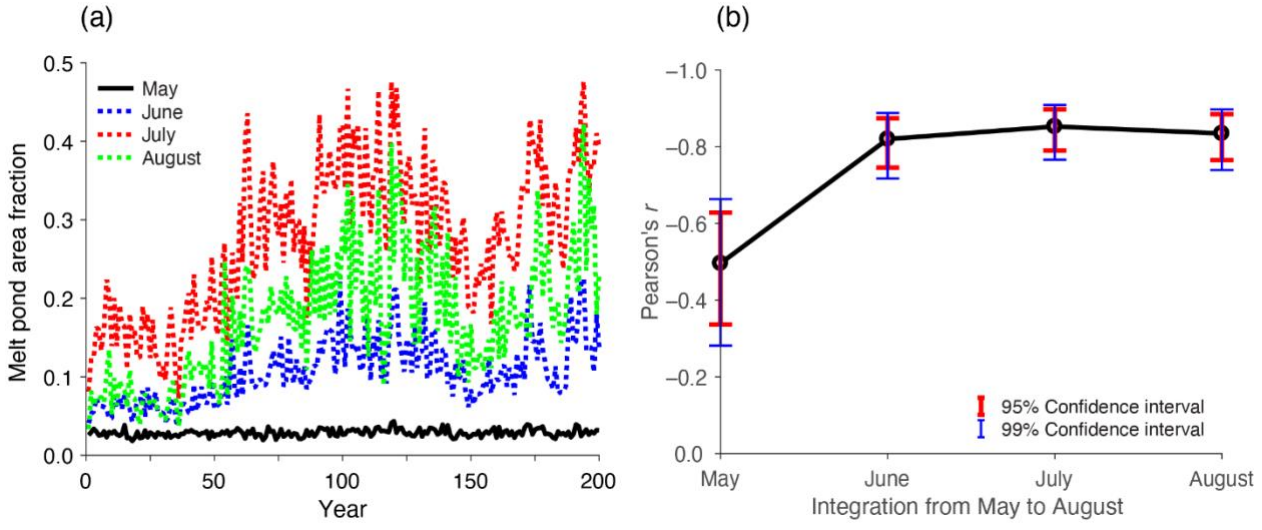

Figure 2: (a) Time series of the modelled melt pond area fraction for May, June, July, and August. (b) Pearson's *r* (with 95% and 99% confidence intervals) between the de-trended time series of the simulated melt pond fraction (integration period from May to August) and modelled September sea ice extent (*N* = 105).

295

https://doi.org/10.5194/egusphere-2023-1560
Preprint. Discussion started: 26 July 2023
© Author(s) 2023. CC BY 4.0 License.

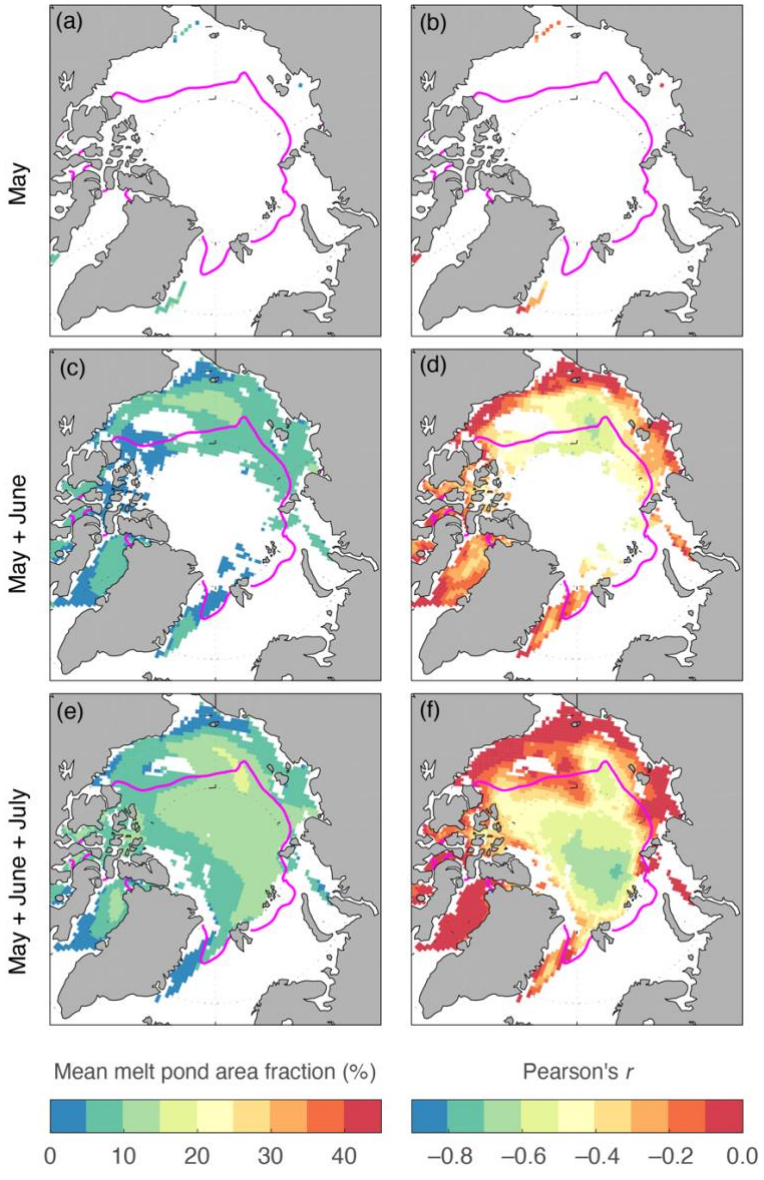

Figure 3: (Left column: a, c, and e) Spatial distribution of mean melt pond area fraction (May through July) from a 105-year simulation conducted with EC-Earth3. (Right column: b, d, and f) Corresponding spatial distribution of correlation between melt pond fraction and de-trended September ice extent (Pearson's $r < 0$) for the selected years of simulation (see Fig. 1a). The magenta line is the mean of modelled September sea ice extent.